COMMUNICATION

Received 00th January 20xx, Accepted 00th January 20xx

DOI: 10.1039/x0xx00000x

Interactions of Emerging Contaminants with Model Colloidal Microplastics, C₆₀ Fullerene, and Natural Organic Matter – Effect of Surface Functional Group and Adsorbate Properties

Tyler Williams, Clare Walsh, Keith Murray, and Mahamud Subir*

Surface adsorption of two commonly detected emerging contaminants, amlodipine (AMP) and carbamazepine (CBZ), onto model colloidal microplastics, natural organic matter (NOM), and fullerene nanomaterials have been investigated. It is found that AMP accumulation at these colloidal-aqueous interfaces is markedly higher than that of CBZ. Measurements of surface excess and particle zeta potential, along with pH-dependent adsorption studies, reveal a distinct influence of colloidal functional group on the adsorption properties of these pharmaceuticals. AMP shows a clear preference for a surface containing carboxylic group compared to an amine modified surface. CBZ, in contrast, exhibit a pH-dependent surface proclivity for both of these microparticles. The type of interactions and molecular differences with respect to structural rigidity and charge properties explain these observed behaviors. In this work, we also demonstrate a facile approach in fabricating uniform microspheres coated with NOM and C₆₀ nanoclusters. Subsequent binding studies on these surfaces show considerable adsorption on the NOM surface but a minimal uptake of CBZ by C60. Adsorption induced colloidal aggregation was not observed. These findings map out the extent of contaminant removal by colloids of different surface properties available in the aquatic environment. The methodology developed for the adsorption study also opens up the possibility for further investigations into colloidalcontaminant interactions.

Introduction

With an increase in consumption and a lack of proper disposal protocol, a wide variety of pharmaceuticals are frequently detected in aquatic ecosystems. It is recognized that conventional remediation techniques remove only a small fraction of these emerging contaminants, leading to their inevitable release to the natural water system. Fig. These compounds can pose potential harm to both humans and aquatic life but to what extent depends on how they interact with colloidal surfaces available in the aquatic

environment. Recent years have also seen a surge in detection of particulate contaminants of emerging concern, which include but not limited to, microplastics $^{10\cdot12}$ and man-made carbon nanomaterials (e.g. C_{60} fullerene $^{13\cdot15}$). Along with naturally occurring particulate organic matter, $^{16\cdot20}$ these colloids can provide sufficient surface area for molecular adsorption and subsequent surface-mediated photo-degradation. Thus, an important pathway by which the distribution and transformation of these pharmaceuticals are altered is their interaction with the surfaces of these particles. $^{16\cdot20}$

Additionally, it is important to elucidate the impact that molecular adsorption can have on the surface charge density of the colloids. Recent studies have shown that hydrodynamic interactions and dye adsorption can lead to colloidal aggregation. 11, 21-23 Adsorption of pharmaceuticals to microplastics, colloidal natural organic matter (NOM), and carbon-based nanomaterials could play a similar role and thereby influence the mobility of these colloidal substances. Given the significance of colloidal surface-contaminant interactions, studies focusing on the association of pharmaceuticals with environmentally relevant colloids are essential. 11-12 However, a practical challenge associated with surface binding studies involving environmental samples is that they often exhibit heterogeneity in size, shape, and the composition of surface chemical functional groups. This is specifically true for microplastics, nanomaterial aggregates, and NOM. To this end, a systematic investigation using particles of uniform size, shape, and known surface functionalities is of fundamental importance and is the focus of this work.

In this communication, we present a surface interactions study of two commonly detected pharmaceuticals,^{2-3, 24} carbamazepine (CBZ), an anticonvulsant drug, and amlodipine (AMP), a calcium channel blocker. These two molecules exhibit distinctive characteristics with respect to molecular rigidity, charge distribution, and chemical moieties they contain. Thus, comparison of their adsorption behaviour can highlight the effect of adsorbate properties on surface interaction. To minimize the uncertainty with respect to particulate heterogeneity and gain fundamental insights into the effect of surface functional groups on the pharmaceutical binding affinity and surface population, we have utilized monodispersed polystyrene (PS) latex microspheres with magnetic core to model different types of surfaces. The findings of this study are presented in two stages. First, we report a pH dependent study of CBZ and AMP adsorption onto bare carboxylic and amine surface functionalized latex particles. These findings highlight the role surface functional groups can play on the adsorption of different classes of pharmaceutical contaminants. There are many studies

a. Address here.

b. Address here.

^{c.} Address here.

[†] Footnotes relating to the title and/or authors should appear here. Electronic Supplementary Information (ESI) available: [details of any supplementary information available should be included here]. See DOI: 10.1039/x0xx00000x

demonstrating the use of PS particles as model microplastics for toxicology and microbial studies.²⁵⁻²⁷ Investigation pertaining to adsorption of pharmaceuticals is limited. Sorption experiments of select emerging contaminants on microplastic debris or large particles (> 250 um) have been reported.²⁸⁻²⁹ However, to the best of our knowledge, the effect of surface functional group on AMP and CBZ adsorption on microplastics in the order of micrometer is not known. Second, we demonstrate the applicability of these magnetic particles in developing a model substrate for studying pharmaceutical interactions with even more complex, heterogeneous surfaces. Colloidal C₆₀ aggregates and Suwannee River NOM (SR-NOM) have been chosen for this purpose. The combined binding studies of CBZ and AMP onto the microplastics and C₆₀ and NOM coated surfaces reveal that surface interaction at the aqueous-colloid interface is intricately dependent not only on the surface functional group of the substrate but also the chemical structure of the pharmaceutical contaminant itself. A schematic diagram of the experimental design and approach is shown in figure

Experimental

Chemicals and materials

Carbamazepine and amlodipine besylate were purchased from Sigma-Aldrich. The chemical structures and UV-Vis spectra of these compounds are shown in figures 1b and 1c. Ultrapure water with resistivity of 18.2 MΩ·cm at 25°C was used in all sample preparation. For pH dependent studies, solutions were prepared using HCI (ACS reagent, 37%) and sodium hydroxide, both purchased from Sigma-Aldrich. The pH of solutions were determined with Thermo-Fisher Scientific benchtop Orion pH meter. The bulk of the research has been carried out using polymeric magnetic particles (MPs) purchased from Bangs Laboratories, Inc. These MPs are iron infused polystyrene (PS) microspheres with carboxyl (ProMag PMC1N) and amine (ProMag PMA1N) surface functional groups. Figure S1 shows a cartoon of the microspheres highlighting the surface functional groups. Experiments, especially those involving C₆₀ surface modifications, were also carried out using amine MPs of similar size (MonoMag, MA1002) obtained from Ocean NanoTech. Particles from both sources yield comparable results.

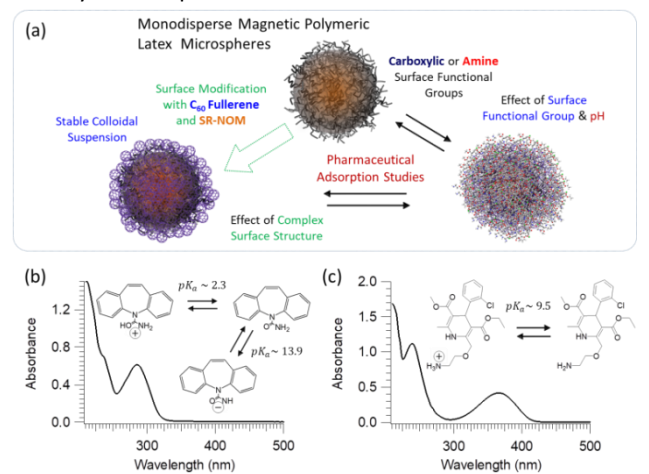


Figure 1 A schematic diagram of the experimental approach (a). UV-Vis spectra (at pH 7), chemical structures, and acid-base chemistry of carbamazepine (b) and amlodipine (c).

The use of magnetic particles is critical as it allows for efficient separation from aqueous medium by means of a

magnetic field. Throughout this article, the amine and the carboxylic MPs are designated as m-PSN and m-PSC, respectively. Both m-PSN and m-PSC display negative ξpotential at all pH solutions studied. In the latter scenario, the source of the negative charge is the de-ionized carboxylic group. In the case of m-PSN, the negative charge is likely due to either or both of the following possibilities - adsorption of anions present in the aqueous medium or the presence of anionic reagents, residing within the polymeric core, used in the post-modification of the polystyrene particles with amine functional group. Suwannee River NOM (Lot No. 2R101N),30 was purchased from the International Humic Substances Society (IHSS). The carboxyl and phenolic content of the SR-NOM have been reported to be 10.4 ± 0.9 meq/(g·C) and 2.9 ± 0.6 meq/(g·C), respectively.30 Phosphate buffered saline (PBS) solution with a pH of 7.4 was used to prepare SR-NOM and C₆₀ solutions. PBS (0.1M) was prepared by mixing appropriate solutions of sodium phosphate dibasic and sodium phosphate monobasic monohydrate (MP Biomedical). These chemicals along with C₆₀ fullerene powder (99%, Alfa Aesar) were purchased from Fisher Scientific. All solutions were prepared using Fisher-brand sterile disposable standard serological pipets and mixed in Class B clear glass threaded vials (polyvinylfaced pulp liner). Quartz and glass cuvettes (1.0 cm) were used to collect UV-Vis spectra and size measurements, respectively. Zetapotential measurements were carried out using disposable folded capillary zeta cell (Malvern Instruments). All glassware was washed with aqua regia (4:1 HCl to HNO₃, Sigma Aldrich).

Preparation of SR-NOM and C₆₀ coated MPs

A stock solution of SR-NOM at a concentration of 300 ppm was prepared by dissolving a known mass into PBS solution with a pH of 7.4. The stock solution has been diluted to 150 ppm in two different 100 mL volumetric flasks where one flask contained a 1:1 ratio by volume of SR-NOM to PBS and the second had a 1:1 ratio by volume of SR-NOM to m-PSN. The final m-PSN density in the mixture was $2.0 \times 10^8 \, mL^{-1}$. A separate m-PSN in PBS was prepared without SR-NOM to serve as a control experiment. Flasks were wrapped in aluminum foil and given 24 hours to equilibrate. Thereafter, stock solutions of m-PSN and the SR-NOM coated particles, which we define as NOM-MP, were separated from the solution by applying a magnetic field for one hour. UV-Vis absorption spectra (Agilent 8453 and UV-1800 Shimadzu UV-Vis spectrometers) of the different concentration of SR-NOM treated with and without m-PSN were collected for a fixed particle density. To ensure the SR-NOM remained bound to the particle surface, the NOM-MP were resuspended in fresh PBS. After resuspension and magnetic separation, UV-Vis spectra of the solution were collected to analyse the extent of SR-NOM desorption. The NOM-MP with optimal surface coverage was used for subsequent AMP and CBZ adsorption studies.

The C_{60} dispersion in water was prepared based on a cosolvent method described in previous studies. $^{31-32}$ Briefly, C_{60} was dissolved in toluene at a concentration of 1mg/mL. Then, it was mixed with water at a 1:4 toluene: water ratio. The mixture was sonicated for approximately 7 hours, swirling every 30 minutes. After sonication, the toluene in the solution was allowed to evaporate under the fume hood for three days to maximize C_{60} solubility. Excess toluene was driven off by purging air into the solution. The aqueous C_{60} dispersion was then passed through a $0.45~\mu m$ nylon filter. This stock solution was stored in dark at room temperature and used to modify m-PSN as needed. UV-Vis absorbance and size measurements showed that C_{60} dispersion

remains stable for at least 4 months. The adsorption of C_{60} onto m-PSN was carried out in PBS solution (pH = 7.4) as described for the adsorption of SR-NOM on MPs. Similarly, concentration dependent characterization of C_{60} adsorption and desorption upon resuspension was also carried out using UV-Vis spectroscopy. The final dispersion, C_{60} -MP (2.0 \times 10⁸ mL^{-1}), was utilized for pharmaceutical adsorption experiments.

Adsorption of pharmaceuticals

To generate adsorption isotherms, prepared stock solutions of the target compound have been used to create two sets of concentration gradients in glass vials. One set was mixed with the appropriate pH or buffer solution and the other was mixed with the desired number density of particles (m-PSN, m-PSC, NOM-MP, or C₆₀-MP). For these experiments, the final particle density, after mixing with the pharmaceutical, was fixed at $1.0 \times 10^8 \, mL^{-1}$. For the bare m-PSN and m-PSC particles, additional isotherms were obtained with particle number densities of 0.5 and 2.0 (\times $10^8)mL^{-1}$. A pH dependent study (4, 7, and 10) was also carried out using the m-PSN and m-PSC colloids. Pharmaceutical adsorption to NOM-MP and C_{60} -MP was conducted in PBS solution. All experiments were carried out at 22 °C. The solution of particles and the molecules were allowed to mix for at least two hours. This ensured adsorption equilibrium had been reached, as determined by time-dependent adsorption study. Magnetic separation method in conjunction with UV-Vis spectroscopy was used to generate adsorption isotherms ($c_{ads} vs. c_{remaining}$ plots), where ccorresponds to the concentration of the target pharmaceutical. At least 20 minutes was given for efficient separation of the magnetic particles. This method has been described in details elsewhere.²³ Briefly, the difference in absorbance of the pharmaceutical compound before $(c_{initial})$ and after $(c_{remaining})$ treating it with the particles was used to determine the concentration of pharmaceuticals adsorbed (c_{ads}) as follows:

$$c_{ads} = c_{initial} - c_{remaining} = \frac{A_{initial} - A_{remaining}}{\epsilon l}$$
 (1)

In this equation, A and ε (in $Lmol^{-1}cm^{-1}$) represent the absorbance and the extinction coefficient of AMP and CBZ at 366 nm ($\varepsilon\sim7\times10^3$) and 285 nm ($\varepsilon\sim1\times10^4$), respectively.

The adsorption isotherms were generated by plotting $c_{ads}\ vs.\ c_{remaining}$. Langmuir (equation 2) isotherm model was used to fit the experimental data. Non-linear least-squares fitting tools in Igor Pro was used for data fitting analysis.

$$c_{ads} = c_{max} \frac{K_{ads} \left(\frac{c_{eq}}{c_0}\right)}{K_{ads} \left(\frac{c_{eq}}{c_0}\right) + 1} \tag{2}$$

The Langmuir fitting parameters are the adsorption constant, K_{ads} , and the maximum surface coverage, c_{max} . It is important to note the use of c_0 in this equation, which denotes the concentration of water (55.5 M), allows the equilibrium constant to be dimensionless and is one of the accurate approaches in obtaining thermodynamic parameters for adsorption processes.³³ The free energy of adsorption is calculated based on the adsorption constant using $\Delta G_{ads} = -RT ln K_{ads}$. This adsorption energy corresponds to the energy released when a molecule goes from an initial state of being solvated to a final state of being bound to the particle surface and is dictated by a number of factors such as electrostatic and hydrophobic interactions. This energy also includes possible rearrangement of the adsorbed molecule, steric

hindrances experienced at the proximity of the surface, and competition with the solvent molecule.

Dynamic Light Scattering Measurements and Infrared Spectroscopy

Colloidal size and zeta potential (ξ) of the particles were determined before (untreated) and after (treated with particles) adsorption of pharmaceuticals. These measurements, which provided pivotal insights into the colloidal stability and charge interactions, were carried out using Zetasizer Nano-ZS, Malvern Instruments. This instrument is equipped with a 4 mW He-Ne laser at wavelength of 633 nm and backscatter detector set at an angle of 173°. Zetasizer was also used to determine the molecular weight of SR-NOM based on the application of Rayleigh scattering and Debye plot. SR-NOM stock was diluted to create a concentration range of 0 - 250 ppm. Solvents were filtered twice through syringes fitted with $0.01 \, \mu m$ filters (Millex-VV PVDF) prior to use. Neat toluene was used as the reference sample. The molecular weight of SR-NOM has been calculated to be $69.4 \pm$ $7.3 \, kDa$. This value is comparable to the molecular weight of colloidal NOM reported earlier.34-35 IR spectra of the SR-NOM, C₆₀, m-PSN particles, and corresponding complexes were collected using attenuated total reflectance Fourier transform infrared (ATR-FTIR) spectrometer (PerkinElmer Frontier, Diamond Zn/Se). SR-NOM and C₆₀ dispersions were dried under N₂ prior to ATR-FTIR measurement. Samples containing magnetic particles (m-PSN, NOM-MP, and C₆₀-MP) were separated, then supernatant removed prior to drying. The data presented is an average of 64 scans at 2 cm⁻¹ resolution, in the range of 700-4000 cm⁻¹. Background spectra (clean surface) were collected prior to the IR measurement of each sample. All spectra were subject to ATR and baseline correction performed by the software provided by the manufacturer.

Results and Discussion

Adsorption of CBZ and AMP on Model Microplastics

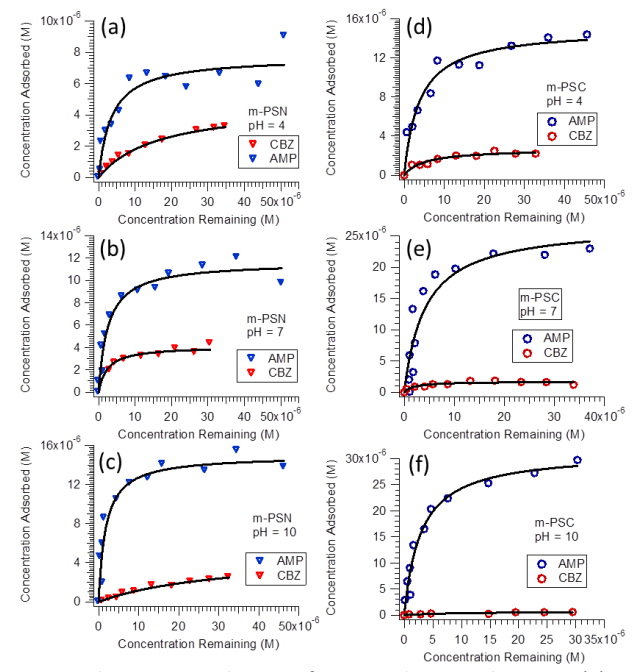


Figure 2 Adsorption isotherms of AMP and CBZ with m-PSN (a) - (c) and m-PSC (d) - (f) at pH 4, 7, and 10. The markers correspond to the experimental data calculated using equation 1 and the solid curve is the Langmuir fit (equation 2). In these experiments the final particle number density is $1.0 \times 10^8 \ mL^{-1}$.

Representative AMP and CBZ adsorption isotherms for the amine and carboxylic surface functionalized particles at different solution pH are shown in figure 2. The Langmuir fit parameters are reported in the Electronic Supplementary Information (ESI) in Table S1. The AMP and CBZ UV-Vis spectra and the corresponding calibration curves are shown in figures S2 and S3, respectively. The results reveal that both AMP and CBZ adsorb at the model microplastic surfaces but their degree of uptake is different for the two distinct surfaces. For instance, irrespective of the solution pH, the c_{max} of AMP for both m-PSN and m-PSC is greater than that of the CBZ. In the case of carboxylic surface, c_{max} of AMP is higher by at least a factor of 5 and this ratio increases with pH.

We have also measured AMP and CBZ adsorption isotherms with different number densities of m-PSC and m-PSN particles. These isotherms are shown in figures S4 and S5, in the ESI. Since ΔG_{ads} only depends on the energetics of the surface interaction, and not on the particle number density, this approach allowed us to obtain an average of $\Delta \textit{G}_{\textit{ads}}$ values (figure 3), with a standard deviation, for a given pharmaceutical-surface interaction. The relatively small standard deviation in the $\Delta \textit{G}_{\textit{ads}}$ values indicates negligible colloidal aggregation.²³ This is further corroborated based on the particle size measurements as discussed below. It is important to note that in all the experiments the particle number density is fixed and the size of m-PSN and m-PSC is known (see figure S6). It is thus possible to calculate the surface excess of the ith species (Γ_i) by dividing c_{max} by the particle surface area and compare this value from one system to the other. This is a clear advantage of utilizing monodispersed and nonporous spherical particles of known number density and size for the adsorption study. The effect of solution pH on Γ_i and the binding affinity, $\Delta \textit{G}_{ads}$, for CBZ and AMP are illustrated in figure 3. The $\Delta \textit{G}_{ads}$ and $\textit{\Gamma}_{i}$ values are an average of 3 adsorption isotherms of different particle densities. The error bars correspond to the standard deviation of the average values.

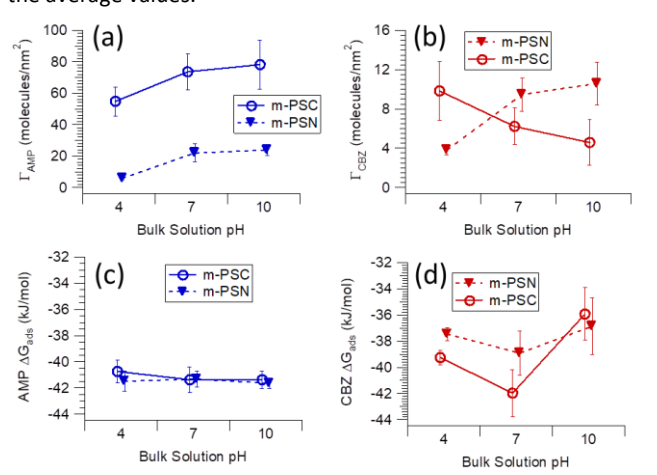


Figure 3 The surface excess, Γ_i , of AMP (a) and CBZ (b), and the Gibbs free energy of adsorption, ΔG_{ads} , of AMP (c) and CBZ (d) as a function of pH.

It is evident that Γ_{AMP} increases with increasing pH for both m-PSC and m-PSN as the adsorbents (figure 3a). Within the pH range studied, the uptake of AMP by the carboxylic functionalized particle is greater than its uptake by the amine functionalized particle. In contrast, Γ_{CBZ} decreases with increasing pH for the m-PSC particles and increases for the m-PSN with increasing pH (figure 3b). It is also important to note that the calculated surface excess is greater than what is expected based on the molecular surface area

of the pharmaceuticals. This is attributed to the fact that the polymeric chains extend out into the aqueous phase from the surface of the sphere and thereby provide a greater effective surface site compared to that of a flat 2-dimensional surface. According to the manufacturer, there are ~50 COOH groups/nm² available on the m-PSC surface. Higher degree of surface coverage has been observed previously for the adsorption of organic dyes on latex particles. ^{23, 36} The implication is that in addition to the specific functional group, extensive van der Waals interaction with the carbon rich polymeric chain available on the particle is expected. In addition to the surface excess values obtained from adsorption isotherms, size and ξ -potential measurements of the particles as a function of the adsorbed pharmaceuticals provide further insights into the adsorption mechanism and colloidal stability. The complete set of size and ξ -potential measurements on these particles for different pH solutions are shown in figure 4. A key finding is that neither AMP nor CBZ adsorption induce colloidal aggregation. Within the measurement standard deviation, the size of the particles remains constant with increasing pharmaceutical concentration. This is true for all the pH conditions studied. Furthermore, it is observed that the ξ -potential of both m-PSC and m-PSN decreases (i.e. the surface becomes less negative) as AMP binds to these particles. In contrast, CBZ binding does not lead to a discernible change in the ξ -potential of these particles.

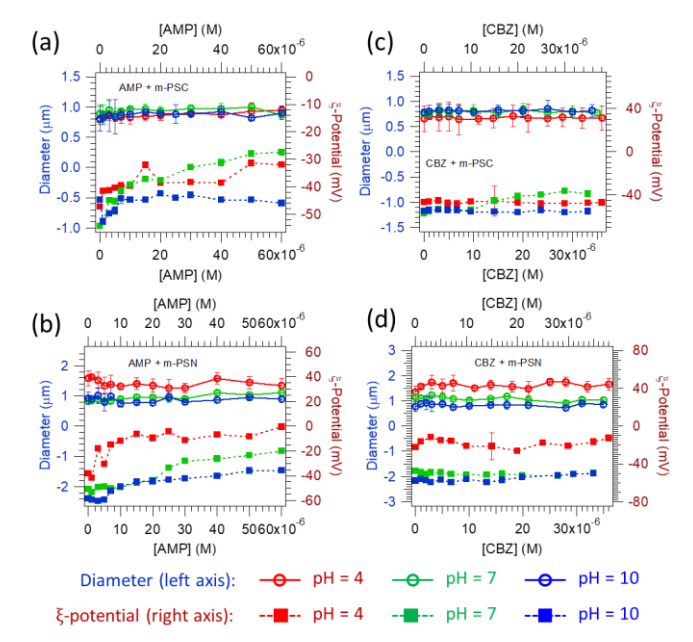


Figure 4 Change in size (left axis) and ξ -potential (right axis) of polymeric particles in the presence of varying pharmaceutical concentration: m-PSC + AMP (a), m-PSN + AMP (b), m-PSC + CBZ (c), and m-PSN + CBZ (d). The pH of the solution is color coded as red = pH 4, green = pH 7, and blue = pH 10.

To interpret these observations, we refer to the pKa values of the pharmaceuticals studied. Within the literature, ^{29, 30} there appears to be two different pKa values (9.5 and 8.6), ³⁷⁻³⁸ reported for AMP. The pKa of 9.5 or higher is likely for AMP since the pKa of ammonium ion is 9.3 and that of protonated primary alkyl ammonium ions are higher. The AMP molecule is thus expected to be positively charged throughout pH 4 and 7 solutions. In fact, we note that the spectra of AMP (figure S2) do not show any change or distortion in its spectral profile as a function of pH except for a slight decrease in the extinction coefficient at 366 nm in pH 10

solution. It is plausible that a new peak is not observed because the neutral species may have a weak absorptivity or that the pKa of AMP is even higher than the theoretical prediction of 9.5. The 366 nm peak is thus representative of the cationic AMP species, which appears to be dominant even in pH 10 solution. Accordingly, It is expected that adsorption of AMP onto the microplastics should make particle ξ -potential less negative. This is clearly observed for all pH solutions. Figures 4a and 4b show that the negative ξ potential of the particles decreases when AMP concentration is increased. The reduction of the negative ξ -potential reaches a plateau with increasing AMP concentration. This behavior is consistent with the surface saturation profile observed in the corresponding adsorption isotherms (figure 2). Based on these observations we conclude that Coulombic attraction play a role on the uptake of AMP onto these negatively charged surfaces. Further evidence to support this conclusion is that AMP surface excess increases with pH. In the case of -COOH functionalized m-PSC, for which the pKa value is around 5,39 increased population of carboxylate ion is expected with increasing pH. Similarly, with an increase in pH, a reduction in the positively charged amine functional groups (pKa ~10),40 minimizing Coulomb repulsion, would lead to a higher uptake of AMP onto m-PSN. This is evident in figure 3a. The electrostatic repulsion from positively charged amine also explains the lower surface population of AMP on m-PSN than that of carboxylic functionalized m-PSC particles.

For CBZ, there is a wide range of pKa values (2.341-42, 743, 13.944, and 15.42) reported in the literature.41-45 There is a lack of clarity with respect to CBZ acid-base chemistry and in certain cases the references cited^{38, 44, 46} are uncorroborated. However, according to a commentary⁴⁷ and the references therein, CBZ exhibits two pKa values, ~2.3 and ~13.9. Based on the acid-base chemistry of similar amides, 48 we deduce these values to correspond to deprotonation of the protonated oxygen and thereafter at the nitrogen (see figure 1b), respectively. The implication is that within the environmental pH range explored in this study, CBZ exists as a neutral species. This explains the observation of unaffected ξ -potential in m-PSC and m-PSN upon CBZ adsorption. Moreover, these measurements, along with the CBZ adsorption isotherm data, reveal that binding of CBZ to the model microplastic surfaces occur even in the absence of pure Coulombic attraction. CBZ uptake on these particles can be described to be predominantly due to van der Waals interaction. Nevertheless, we note that the CBZ uptake is influenced by the type of surface functional group and responsive to the pH change (fig. 3b). We surmise that this is likely due to the properties of the microparticle surface itself. One possibility is that protonation/deprotonation of these interfacial functional groups could modulate the effective surface site by causing the polystyrene chain to expand or collapse and thereby be more or less accessible to CBZ. This is an important finding that goes to show that even in the case of primarily hydrophobic or van der Waals interaction, colloidal surface charge can play a role on the overall uptake of pharmaceutical contaminants.

Next, we turn to the discussion of adsorption affinity as dictated by the ΔG_{ads} values. Within the experimental uncertainty, ΔG_{ads} for AMP is not affected by the compositions of the colloidal surface and pH of the solution (figure 3c). Yet, if Coulombic attraction is to a play a role, a higher binding affinity for the positively charged AMP toward the negatively charged carboxylate particle would be anticipated. CBZ appears to show a slight variation in its ΔG_{ads} ; however, these values are comparable when we take into account of the standard deviation. These observations indicate that the interaction of these pharmaceuticals with the

model microplastics are occurring at a surface that is energetically homogeneous. Based on the surface excess values, we know that van der Waals interaction with the polymeric carbon is extensive. The similarity in the ΔG_{ads} values could also be a consequence of the fact that, unlike adsorption from vacuum to a clean surface, the Gibbs free energy of adsorption at an aqueous-solid interface includes multiple contributions⁴⁹⁻⁵¹ including, but not limited to, pure electrostatic, hydrophobic interactions, $\pi - \pi$ interactions, hydrogen bonding and solvation. These forces can have a balancing effect. 50, 52 For instance, the negatively charged m-PSC particle at higher pH is likely to be more strongly hydrated compared to the particles dispersed in neutral to acidic pH. The energetics of displacing water molecule can counter the driving force of adsorption due to Coulombic attraction. Thus, for physisorption of a solute from an aqueous solution, a similar overall free energy of adsorption is possible. This has been observed for a cationic dye adsorption on latex particles and also for adsorption of particles onto the oil-water interface. 50, 52 Accordingly, it is not possible to isolate the specific interaction AMP and CBZ exhibit on these surfaces solely based on the ΔG_{ads} values.

Nevertheless, a comparison of the surface coverage suggests that both the molecular structure of the adsorbate and the microplastic surface functional group have an impact on the uptake of these contaminants. This is illustrated by the AMP-to-CBZ surface excess ratio, $\frac{\Gamma_{AMP}}{\Gamma_{CBZ}}$ (Table 1), for the different substrates. For instance, the ratio is greater than 1 for both m-PSC and m-PSN. That is, CBZ exhibits a lesser degree of uptake regardless of the surface composition. We attribute this to the differences in the geometry and the rigidity of these molecules. AMP, which has about 10 rotatable bonds,⁵³ is much more flexible to adsorb onto the polymeric latex particle surface. In contrast, with no rotatable bond, CBZ is rigid and thus can have limited access to the polymeric surface. Comparison of these ratios also suggest that a greater extent of uptake of AMP, relative to CBZ, occurs on surfaces containing acidic carboxylic functional group compared to the surfaces of basic functional group such as amine. This can be attributed to the fact that AMP exhibits Coulombic attraction and CBZ molecules do not. Certainly, this is supported by the increase in surface excess ratio with increasing pH. However, other favorable interactions at the amine-aqueous interface, such as hydrogen bonding or enhanced hydration effect, that can augment CBZ binding sites, cannot be ruled out. For example, enhanced CBZ interaction with Pahokee peat NOM sorbent due to hydration effect has previously been reported.20

Table 1 The surface excess ratios, $\frac{\Gamma_{AMP}}{\Gamma_{CBZ}}$, for different substrates

Substrate	$rac{\Gamma_{AMP}}{\Gamma_{CBZ}}$ Ratio
m-PSC (<i>Polystyrene,</i> - <i>COOH</i> /- <i>COO</i> ⁻)	5.6 ± 1.1 at pH 4
	11.8 ± 2.1 at pH 7
	17.0 ± 5.3 at pH 7
$ m-PSN \\ (Polystyrene, \\ -NH_2/-NH_3^+) $	1.6 ± 0.2 at pH 4
	2.3 ± 0.6 at pH 7
	2.3 ± 0.4 at pH 10

NOM-MP (carboxylic, phenolic, etc.)	4. 4 ± 1.9 (pH 7.4, PBS)
$C_{60} ext{-MP}$ (π electrons, $-\mathit{OH}$, etc.)	13. 0 ± 3.8 (pH 7.4, PBS)

Adsorption of CBZ and AMP on NOM-MP and C₆₀-MP

In this section, we first demonstrate that latex particles can be coated with NOM and carbon-based nanomaterials. The use of magnetic micropspheres that are uniform in size brings multiple practical and scientific advantages. For example, they can be effectively separated from the aqueous solution and since their size and number densities are known, they allow the calculation of adsorbate surface excess in terms of molecules per area. As shown in the previous section, these values can map out the effect of surface functional group on the extent of adsorbate uptake. We begin by presenting the results of SR-NOM and C_{60} coated m-PSN particle preparation and then discuss the adsorption properties of AMP and CBZ onto the model NOM and C_{60} surfaces.

The details of NOM-MP (m-PSN particles coated with SR-NOM) and C_{60} -MP (m-PSN particles coated with C_{60}) are given in the experimental section. It is found that both SR-NOM and C_{60} spontaneously adsorbs onto the m-PSN particles when mixed in PBS solution. Figure 5a shows that for a given initial concentration of SR-NOM, its absorbance is lower when treated with the m-PSN particles, meaning SR-NOM has been taken up by the m-PSN. The spectra of SR-NOM after resuspension (red trace) corresponds to the fresh PBS solution in which NOM-MP was re-dispersed, allowed to equilibrate for at least an hour, and then separated using a magnetic field. The absorbance is negligible, suggesting that only few molecules, if any, of SR-NOM came off the particles. Multiple resuspensions of the NOM-MP in subsequent fresh PBS solution showed no further desorption of SR-NOM.

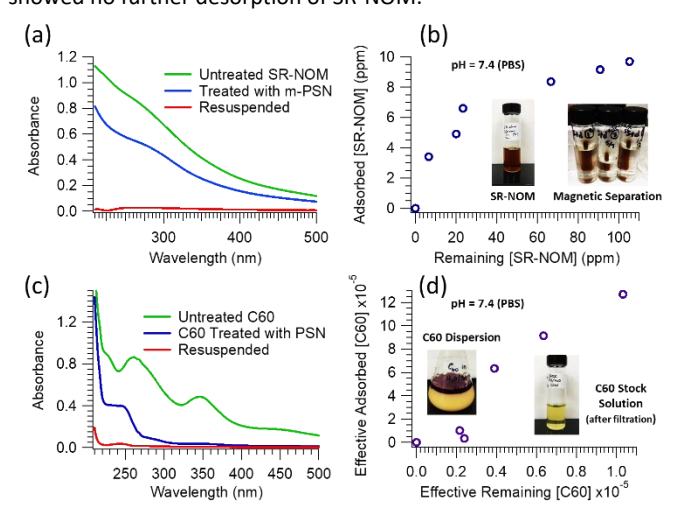


Figure 5 (a) UV-Vis absorption spectra of SR-NOM before and after treating with a fixed number density of m-PSN. The effect of resuspending the modified NOM-MP is also shown (b) Adsorption isotherm of SR-NOM onto m-PSN. The insets show the photographs of the stock SR-NOM solution and that of the magnetic separated SR-NOM and m-PSN mixtures. The similar aspects of C_{60} adsorption onto m-PSN are presented in (c) and (d). The insets in (d) show the C_{60} dispersion before and after filtration.

The difference in the absorbance values of SR-NOM at 290 nm has been used to plot the amount of SR-NOM adsorbed as a function of its equilibrium concentration remaining in the solution (Fig. 5b). The plateau suggests a saturated surface coverage. At the highest concentration level, the SR-NOM adsorbed is approximately 10 ppm. With the knowledge of the molecular weight of the colloidal SR-NOM and the size of these colloids (shown in figure S7), the estimated number of SR-NOM particles adsorbed on the m-PSN surface is 6.4×10^{16} particles per m². This corresponds to an area of approximately $16 nm^2$ for a given SR-NOM, assuming spherical particles, deposited on m-PSN. This is about 10^4 order of magnitude smaller than the area occupied by a single SR-NOM particle. The implication is that the SR-NOM is attached to the three-dimensional (3D) polystyrene chains of the latex bead protruding into the aqueous phase from the particle surface. The behavior is similar to the adsorption of protein on 3D interphase between the bulk solution and the physical adsorbent surface.⁵¹ Further evidence of surface coating of SR-NOM comes from IR spectroscopy. ATR-FTIR spectrum of NOM-MP (Fig. 6) shows signature peaks observed in the fingerprint region of the aqueous dispersion of SR-NOM. Additionally, a broad band around 2500 cm⁻ ¹, like the IR band in powder SR-NOM (Fig. S8), is also evident.

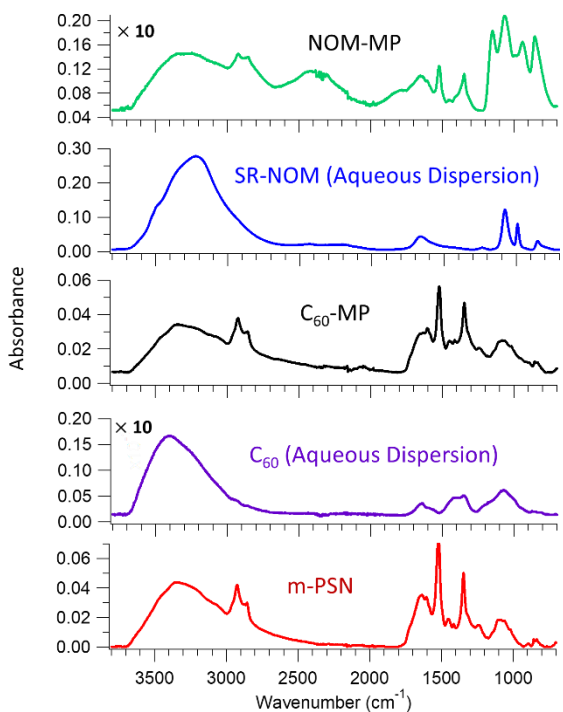


Figure 6 ATR-FTIR spectra of microplastics, C_{60} , SR-NOM, and the corresponding surface modified colloids. Due to weak absorbance, select spectra have been magnified ten-fold ($\times 10$).

For the subsequent pharmaceutical adsorption studies, NOM-MP prepared using the highest possible SR-NOM concentration has been used. The photographs in figure 5b provide visual description of the SR-NOM dispersion and the magnetic separation process. Evidence of its stable colloidal nature is given in figure S7 in terms of size and zeta potential measurements. Figures 5c and 5d were generated in a similar fashion as described above except that they represent the adsorption process of C_{60} fullerene nanoparticles onto m-PSN. These data reveal that C_{60} also binds strongly to the m-PSN and does not desorb upon resuspension. A plot of the amount of C_{60} adsorbed (Fig. 5d) has been generated using C_{60} absorbance

peak at 348 nm. Effective concentrations for each sample have been calculated based on the C_{60} extinction coefficient at 348 nm. The photograph of C_{60} dispersion contained in the Erlenmeyer flask (Fig. 5d) shows the purple toluene (top) layer containing C_{60} that is removed by filtration after allowing the toluene to evaporate. The final product, after filtration, labeled as the C_{60} stock solution after filtration is also shown. ATR-FTIR spectrum of C_{60} -MP (Fig. 6) shows peak broadening and elevated baseline in the range of 800 – 1800 cm⁻¹, indicating the presence of C_{60} . Unlike SR-NOM, C_{60} aggregates exhibit weak absorption coefficients and peaks strongly overlapping with that of m-PSN. These factors make it difficult to directly characterize C_{60} aggregates on m-PSN. Figure S8 shows the IR spectrum of C_{60} powder.

These stable surface modified NOM-MP and C_{60} -MP were used for AMP and CBZ adsorption studies. Figures 7a and 7b show the adsorption isotherms of AMP and CBZ on NOM-MP and C_{60} -MP, respectively. Replicates of adsorption isotherms are provided in the ESI (figure S9) and the average Langmuir fit parameters of two independent trials are reported in Table S2. Control experiments with adsorption of AMP and CBZ onto the surrogate m-PSN particles in 0.1 M PBS solution have also been carried out. The corresponding adsorption isotherms are shown in the ESI (figure S10). It is evident from figure 7 that AMP shows propensity for both NOM-MP and the C_{60} -MP surfaces. While CBZ adsorbs on NOM-MP, its uptake by C_{60} -MP is negligible.

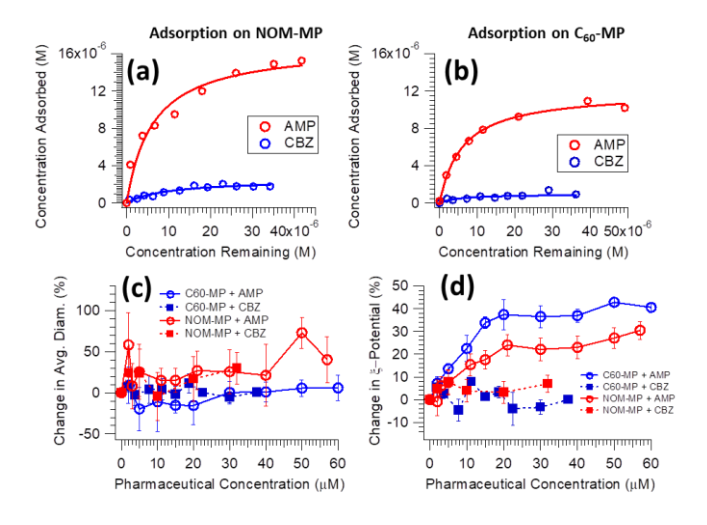


Figure 7 Adsorption isotherms of AMP and CBZ onto NOM-MP (a) and C_{60} -MP (b). The markers represent experimental data, and the solid traces represent the Langmuir fits. The percentage change in size (c) and ξ -potential upon adsorption of AMP and CBZ (d).

The ΔG_{ads} and c_{max} values obtained for these surfaces are distinct from those obtained in the control experiment using m-PSN particles (Table S3). AMP exhibits a similar binding affinity for the SR-NOM and C₆₀ surfaces ($\Delta G_{ads} \sim -40 kJ/mol$), which is comparable to its binding affinity toward carboxylic and amine functionalized microparticles. In contrast, CBZ shows slightly higher affinity for the C₆₀ surface compared to that of NOM (see Table S2). Not a significant difference is observed in ΔG_{ads} of AMP with variation in surface composition. As discussed earlier, this is likely for physisorption from aqueous solution arising from balancing out of different contributions toward adsorption free energy where van der Waals interaction is also dominant.

It is observed that compared to C₆₀-MP, NOM-MP can facilitate higher uptake of both AMP and CBZ. This we attribute to the polymeric structure of SR-NOM, which can extend into the aqueous phase increasing the effective surface sites with which the pharmaceuticals can interact. The chemical structure of NOM includes hydrophobic, hydrophilic, and charged surfaces. $^{54\text{-}56}$ In addition to polymeric carbon chain, the particular Suwannee River NOM used in this study is rich in carboxylic and phenolic functional groups. On the other hand, C₆₀-MP provide a surface that is hydrophobic and susceptible to interactions with its π -orbitals.⁵⁷ Due to surface curvature and their size, these aggregates exhibit hydrophobic characteristics. 58-59 However, the C₆₀ clusters dispersed in water also undergo surface hydroxylation³¹⁻³² and OH⁻ ions can accumulate at the water-hydrophobic interfaces and stabilize the hydrophobic colloidal substances. 60-62 Thus, in addition to the hydrophobic interaction, electrostatic attraction is plausible in the case of AMP. The negative ξ -potential measured for C₆₀ colloids and C₆₀-MP (figure S7) is likely due to adsorption of OH⁻ or phosphate ions on these surfaces.

Figures 7c and 7d show the effect of pharmaceutical adsorption on the size and ξ -potential of NOM-MP and C₆₀-MP. The data is presented as percentage change in reference to the size or ξ -potential of the particles in the absence of pharmaceuticals. The raw data, which show the absolute size and ξ -potential values are shown in figure S11 of the ESI. It is apparent (Fig. 7c) that within the experimental error, the size of these particles remains relatively unchanged as a function of pharmaceutical concentration. While a large standard deviation is observed, indicating that a certain fraction of these particles is coalescing, an increase in the average particle size greater than hundred percent is not seen. Thus, aggregates composed of two or more particles are not prominent. As expected, we also see adsorption of AMP diminishes the ξ potential, whereas adsorption of neutral CBZ does not. Coulomb interaction between the positively charged AMP and the negatively charged surface of these particles is one of the driving forces of AMP adsorption. As with adsorption on the model microplastics, comparison of $\frac{\varGamma_{AMP}}{\varGamma_{CBZ}}$ ratios for these surfaces, also demonstrate greater extent of uptake for AMP. It is interesting to note that at the SR-NOM surface, this ratio falls between that of the amine and carboxylic functionalized particles. It is plausible that similar to the basic $-NH_2$ moiety, the phenolic -OH group may limit the adsorption site for CBZ. The same effect may also explain a substantially reduced uptake of CBZ on the C60-MP surface, which is likely to contain hydroxylated sites and hydroxide ions.

Conclusions

In this communication, we presented a systematic surface adsorption study of two commonly detected pharmaceutical contaminants, namely CBZ and AMP, onto model microplastics, colloidal SR-NOM, and C₆₀ fullerene. The effect of pH on the surface excess and binding strength of these pharmaceuticals on the polystyrene particles of distinct surface functional groups (amine vs. carboxylic) has been highlighted. Based on surface excess ratios, a clear picture has emerged – on all the substrates studied, AMP, which exists in its cationic form within the pH range investigated, exhibits a greater degree of uptake compared to CBZ. Attractive coulombic interaction and greater degrees of rotational freedom in AMP can explain the observed differences. Comparing the AMP surface excess, the extent of uptake by

the substrates near neutral pH can be ranked as follows $COOH/COO^-\gg NH_2/NH_3^+$ at pH 7 and $SR-NOM>C_{60}$ at pH 7.4 in PBS buffer. For CBZ, the order of uptake is $COOH/COO^-\sim NH_2/NH_3^+$ at pH 7 and $SR-NOM\gg C_{60}$, with significantly diminished uptake on C_{60} nanomaterials. Thus, this study demonstrated that there can be a clear surface effect on the amount of pharmaceuticals adsorbed on microplastics and other colloidal substances ubiquitous in the aquatic environment. To elucidate specific binding interactions, further computational and surface selective spectroscopic investigations are needed.

Within this study, we have also shown that model colloidal substrates composed of natural organic matter and carbon-based nanomaterials can be designed to investigate the influence of specific functional groups on surface interactions of emerging contaminants. Previous studies have shown the potential interactions of humic acids and NOM with minerals, non-magnetic polymeric substances, and engineered nanoparticles.63-66 Application of magnetic particles and other designer nanomaterials for the purpose of pollution remediation has also been demonstrated.⁶⁷⁻⁷⁰ However, the design and fabrication of NOM or C₆₀ coated magnetic polymeric colloids, for the purpose of further pharmaceutical binding studies, have yet to be reported. The use of monodispersed spherical surrogate particles of well characterized size and surface properties opens up the possibility for further spectroscopic investigations. For instance, stable particles of homogeneous size and shape are required for vibrational sum frequency and second harmonic generation spectroscopy techniques.71-74 These tools can elucidate the much needed understanding of pharmaceutical-NOM interactions at the molecular level and would be made possible by the model colloids described herein.

Conflicts of interest

There are no conflicts to declare.

Acknowledgement

This material is based upon work supported by the National Science Foundation under Grant No. 1808468. We also acknowledge the support provided by the Ball State ASPIRE Junior Faculty Research and the Indiana Academy of Science Grants.

References

- 1. Kümmerer, K., Pharmaceuticals in the Environment. *Annual Review of Environment and Resources* **2010**, *35*, 57-75.
- 2. Domènech, X.; Ribera, M.; Peral, J., Assessment of Pharmaceuticals Fate in a Model Environment. *Water, Air, & Soil Pollution* **2011**, *218*, 413-422.
- 3. Padhye, L. P.; Yao, H.; Kung'u, F. T.; Huang, C.-H., Year-Long Evaluation on the Occurrence and Fate Of pharmaceuticals, Personal Care Products, And endocrine Disrupting Chemicals

- in an Urban Drinking Water Treatment Plant. Water Research 2014, 51, 266-276.
- Snyder, S. A.; Westerhoff, P.; Yoon, Y.; Sedlak, D. L., Pharmaceuticals, Personal Care Products, and Endocrine Disruptors in Water: Implications for the Water Industry. *Environmental Engineering Science* 2003, 20, 449-469.
- Kostich, M. S.; Batt, A. L.; Lazorchak, J. M., Concentrations of Prioritized Pharmaceuticals in Effluents from 50 Large Wastewater Treatment Plants in the Us and Implications for Risk Estimation. *Environmental Pollution* 2014, 184, 354-359.
- Dalrymple, O. K.; Yeh, D. H.; Trotz, M. A., Removing Pharmaceuticals and Endocrine-Disrupting Compounds from Wastewater by Photocatalysis. *Journal of Chemical Technology and Biotechnology* 2007, 82, 121-134.
- Ross, I.; McDonough, J.; Miles, J.; Storch, P.; Thelakkat Kochunarayanan, P.; Kalve, E.; Hurst, J.; S. Dasgupta, S.; Burdick, J., A Review of Emerging Technologies for Remediation of Pfass. *Remediation Journal* 2018, 28, 101-126.
- Amin, N. A. S.; Shahzad, K., A Review on Removal of Pharmaceuticals from Water by Adsorption Au - Akhtar, Javaid. *Desalination and Water Treatment* 2016, 57, 12842-12860.
- Archer, E.; Petrie, B.; Kasprzyk-Hordern, B.; Wolfaardt, G. M., The Fate of Pharmaceuticals and Personal Care Products (Ppcps), Endocrine Disrupting Contaminants (Edcs), Metabolites and Illicit Drugs in a Wwtw and Environmental Waters. Chemosphere 2017, 174, 437-446.
- 10. Lambert, S.; Wagner, M., Microplastics Are Contaminants of Emerging Concern in Freshwater Environments: An Overview. In Freshwater Microplastics: Emerging Environmental Contaminants?, Wagner, M.; Lambert, S., Eds. Springer International Publishing: Cham, 2018; pp 1-23.
- Alimi, O. S.; Farner Budarz, J.; Hernandez, L. M.; Tufenkji, N., Microplastics and Nanoplastics in Aquatic Environments: Aggregation, Deposition, and Enhanced Contaminant Transport. Environmental Science & Technology 2018, 52, 1704-1724.
- Wang, J.; Liu, X.; Li, Y.; Powell, T.; Wang, X.; Wang, G.; Zhang, P., Microplastics as Contaminants in the Soil Environment: A Mini-Review. Science of The Total Environment 2019, 691, 848-857.
- Freixa, A.; Acuña, V.; Gutierrez, M.; Sanchís, J.; Santos, L. H. M. L. M.; Rodriguez-Mozaz, S.; Farré, M.; Barceló, D.; Sabater, S., Fullerenes Influence the Toxicity of Organic Micro-Contaminants to River Biofilms. Frontiers in Microbiology 2018, 9.
- 14. Sanchís, J.; Milačič, R.; Zuliani, T.; Vidmar, J.; Abad, E.; Farré, M.; Barceló, D., Occurrence of C60 and Related Fullerenes in the Sava River under Different Hydrologic Conditions. Science of The Total Environment 2018, 643, 1108-1116.
- Farré, M.; Pérez, S.; Gajda-Schrantz, K.; Osorio, V.; Kantiani, L.; Ginebreda, A.; Barceló, D., First Determination of C60 and C70 Fullerenes and N-Methylfulleropyrrolidine C60 on the Suspended Material of Wastewater Effluents by Liquid Chromatography Hybrid Quadrupole Linear Ion Trap Tandem Mass Spectrometry. *Journal of Hydrology* 2010, 383, 44-51.
- Philippe, A.; Schaumann, G. E., Interactions of Dissolved Organic Matter with Natural and Engineered Inorganic Colloids: A Review. *Environmental Science & Technology* 2014, 48, 8946-8962.

- Navon, R.; Hernandez-Ruiz, S.; Chorover, J.; Chefetz, B., Interactions of Carbamazepine in Soil: Effects of Dissolved Organic Matter. *Journal of Environmental Quality* 2011, 40, 942-948.
- Deshusses, M. A., Adsorption of Clofibric Acid and Ketoprofen onto Powdered Activated Carbon: Effect of Natural Organic Matter Au - Gao, Yaohuan. *Environmental Technology* 2011, 32, 1719-1727.
- Artifon, V.; Zanardi-Lamardo, E.; Fillmann, G., Aquatic Organic Matter: Classification and Interaction with Organic Microcontaminants. Science of The Total Environment 2019, 649, 1620-1635
- Borisover, M.; Sela, M.; Chefetz, B., Enhancement Effect of Water Associated with Natural Organic Matter (Nom) on Organic Compound–Nom Interactions: A Case Study with Carbamazepine. Chemosphere 2011, 82, 1454-1460.
- Szilagyi, I.; Trefalt, G.; Tiraferri, A.; Maroni, P.; Borkovec, M., Polyelectrolyte Adsorption, Interparticle Forces, and Colloidal Aggregation. Soft Matter 2014, 10, 2479-2502.
- Kovalchuk, N. M.; Starov, V. M., Aggregation in Colloidal Suspensions: Effect of Colloidal Forces and Hydrodynamic Interactions. Advances in Colloid and Interface Science 2012, 179-182, 99-106.
- 23. Williams, T. A.; Lee, J.; Diemler, C. A.; Subir, M., Magnetic Vs. Non-Magnetic Colloids a Comparative Adsorption Study to Quantify the Effect of Dye-Induced Aggregation on the Binding Affinity of an Organic Dye. *Journal of Colloid and Interface Science* **2016**, *481*, 20-27.
- 24. Saari, G. N.; Scott, W. C.; Brooks, B. W., Global Scanning Assessment of Calcium Channel Blockers in the Environment: Review and Analysis of Occurrence, Ecotoxicology and Hazards in Aquatic Systems. *Chemosphere* 2017, 189, 466-478.
- 25. Galgani, L.; Engel, A.; Rossi, C.; Donati, A.; Loiselle, S. A., Polystyrene Microplastics Increase Microbial Release of Marine Chromophoric Dissolved Organic Matter in Microcosm Experiments. Scientific Reports 2018, 8, 14635.
- 26. Stock, V., et al., Uptake and Effects of Orally Ingested Polystyrene Microplastic Particles in Vitro and in Vivo. *Archives of Toxicology* **2019**, *93*, 1817-1833.
- Hesler, M., et al., Multi-Endpoint Toxicological Assessment of Polystyrene Nano- and Microparticles in Different Biological Models in Vitro. *Toxicology in Vitro* 2019, 61, 104610.
- 28. Seidensticker, S.; Grathwohl, P.; Lamprecht, J.; Zarfl, C., A Combined Experimental and Modeling Study to Evaluate Ph-Dependent Sorption of Polar and Non-Polar Compounds to Polyethylene and Polystyrene Microplastics. *Environmental Sciences Europe* **2018**, *30*, 30.
- Wu, C.; Zhang, K.; Huang, X.; Liu, J., Sorption of Pharmaceuticals and Personal Care Products to Polyethylene Debris. *Environmental Science and Pollution Research* 2016, 23, 8819-8826.
- 30. Driver, S. J.; Perdue, E. M., Acidic Functional Groups of Suwannee River Natural Organic Matter, Humic Acids, and Fulvic Acids. In Advances in the Physicochemical Characterization of Dissolved Organic Matter: Impact on Natural and Engineered Systems, American Chemical Society: 2014; Vol. 1160, pp 75-86.
- Brant, J. A.; Labille, J.; Bottero, J.-Y.; Wiesner, M. R., Characterizing the Impact of Preparation Method on Fullerene Cluster Structure and Chemistry. *Langmuir* 2006, 22, 3878-3885.

- Labille, J.; Masion, A.; Ziarelli, F.; Rose, J.; Brant, J.; Villiéras, F.; Pelletier, M.; Borschneck, D.; Wiesner, M. R.; Bottero, J.-Y., Hydration and Dispersion of C60 in Aqueous Systems: The Nature of Water–Fullerene Interactions. *Langmuir* 2009, 25, 11232-11235.
- Tran, H. N.; You, S.-J.; Hosseini-Bandegharaei, A.; Chao, H.-P., Mistakes and Inconsistencies Regarding Adsorption of Contaminants from Aqueous Solutions: A Critical Review. Water Research 2017, 120, 88-116.
- 34. B. Wagoner, D.; F. Christman, R., Molar Mass and Size of Suwannee River Natural Organic Matter Using Multi-Angle Laser Light Scattering, 1997; Vol. 31.
- 35. Wagoner, D. B.; Christman, R. F., Molar Mass and Size of Norwegian Aquatic Nom by Light Scattering. *Environment International* **1999**, *25*, 275-284.
- Charreyre, M.-T.; Zhang, P.; Winnik, M. A.; Pichot, C.; Graillat,
 C., Adsorption of Rhodamine 6g onto Polystyrene Latex
 Particles with Sulfate Groups at the Surface. *Journal of Colloid and Interface Science* 1995, 170, 374-382.
- 37. Kaynak, M.; Bogacz, A.; Stelmasin´ Ski, M.; Sahin, S., Bioavailability File: Amlodipine, 2011; Vol. 36, p 207-222.
- 38. Yoshida, F.; Topliss, J. G., Qsar Model for Drug Human Oral Bioavailability. *Journal of Medicinal Chemistry* **2000**, *43*, 2575-2585.
- Subir, M.; Liu, J.; Eisenthal, K. B., Protonation at the Aqueous Interface of Polymer Nanoparticles with Second Harmonic Generation. *The Journal of Physical Chemistry C* 2008, 112, 15809-15812.
- 40. Zhao, X.; Ong, S.; Wang, H.; Eisenthal, K. B., New Method for Determination of Surface Pka Using Second Harmonic Generation. Chemical Physics Letters 1993, 214, 203-207.
- 41. Nghiem, L. D.; Schäfer, A. I.; Elimelech, M., Pharmaceutical Retention Mechanisms by Nanofiltration Membranes. *Environmental Science & Technology* **2005**, *39*, 7698-7705.
- Hernandez-Ruiz, S.; Abrell, L.; Wickramasekara, S.; Chefetz, B.; Chorover, J., Quantifying Ppcp Interaction with Dissolved Organic Matter in Aqueous Solution: Combined Use of Fluorescence Quenching and Tandem Mass Spectrometry. Water Research 2012, 46, 943-954.
- 43. Bai, Y.; Wu, F.; Liu, C.; Guo, J.; Fu, P.; Li, W.; Xing, B., Interaction between Carbamazepine and Humic Substances: A Fluorescence Spectroscopy Study. *Environmental Toxicology and Chemistry* 2008, 27, 95-102.
- 44. Jones, O. A. H.; Voulvoulis, N.; Lester, J. N., Aquatic Environmental Assessment of the Top 25 English Prescription Pharmaceuticals. *Water Research* **2002**, *36*, 5013-5022.
- 45. Jjemba, P. K., Excretion and Ecotoxicity of Pharmaceutical and Personal Care Products in the Environment. *Ecotoxicology and Environmental Safety* **2006**, *63*, 113-130.
- 46. Comprehensive Medicinal Chemistry. The Rational Design, Mechanistic Study and Therapeutic Application of Chemical Compounds. 6 Bände. Herausgegeben Von C. Hansch, P. G. Sammes Und J. B. Taylor. Pergamon Press, Oxford 1990. Geb. \$ 1995.00 (Einzelband: \$ 350.00). Isbn (Gesamtwerk) 0-08-032530-0. Angewandte Chemie 1991, 103, 341-341.
- 47. Bui, T. X.; Choi, H., Comment on "Adsorption and Desorption of Oxytetracycline and Carbamazepine by Multiwalled Carbon Nanotubes". *Environmental Science & Technology* **2010**, *44*, 4828-4828.
- 48. Roberts, J. D.; Caserio, m. C., Basic Principles of Organic Chemistry; W. A. Benjamin, Inc.: Menlo Park, 1977.

- 49. Somasundaran, P.; Shrotri, S.; Huang, L., Thermodynamics of Adsorption of Surfactants at Solid-Liquid Interface. In *Pure and Applied Chemistry*, 1998; Vol. 70, p 621.
- 50. Eckenrode, H. M.; Jen, S.-H.; Han, J.; Yeh, A.-G.; Dai, H.-L., Adsorption of a Cationic Dye Molecule on Polystyrene Microspheres in Colloids: Effect of Surface Charge and Composition Probed by Second Harmonic Generation. *The Journal of Physical Chemistry B* 2005, 109, 4646-4653.
- 51. Vogler, E. A., Protein Adsorption in Three Dimensions. *Biomaterials* **2012**, *33*, 1201-1237.
- 52. Wu, W.; Liu, X.; Chen, S.-L.; Yuan, Q.; Gan, W., Particle Adsorption at the Oil–Water Interface Studied with Second Harmonic Generation. *Soft Matter* **2019**, *15*, 7672-7677.
- 53. Wishart, D. S.; Knox, C.; Guo, A. C.; Shrivastava, S.; Hassanali, M.; Stothard, P.; Chang, Z.; Woolsey, J., . Drugbank: a comprehensive resource for in silico drug discovery and exploration. Nucleic Acids Res. 2006 Jan 1, 34 (Database issue): D668-72. 16381955.
- 54. Zhang, D.; Duan, D.; Huang, Y.; Yang, Y.; Ran, Y., Composition and Structure of Natural Organic Matter through Advanced Nuclear Magnetic Resonance Techniques. *Chemical and Biological Technologies in Agriculture* **2017**, *4*, 8.
- 55. Guo, L.; Lehner, J. K.; White, D. M.; Garland, D. S., Heterogeneity of Natural Organic Matter from the Chena River, Alaska. *Water Research* **2003**, *37*, 1015-1022.
- 56. Uyguner Demirel, C.; Bekbolet, M.; Swietlik, J., Natural Organic Matter: Definitions and Characterization, 2007, p 253-277.
- 57. Keiluweit, M.; Kleber, M., Molecular-Level Interactions in Soils and Sediments: The Role of Aromatic Π-Systems. *Environmental Science & Technology* **2009**, *43*, 3421-3429.
- 58. Sun, Q.; Su, X. W.; Cheng, C. B., The Dependence of Hydrophobic Interactions on Solute Size. *Chemical Physics* **2019**, *516*, 199-205.
- 59. Zangi, R., Are Buckyballs Hydrophobic? *The Journal of Physical Chemistry B* **2014**, *118*, 12263-12270.
- 60. Ma, A.; Xu, J.; Xu, H., Impact of Spontaneously Adsorbed Hydroxide Ions on Emulsification Via Solvent Shifting. The Journal of Physical Chemistry C 2014, 118, 23175-23180.
- 61. Gan, W.; Wu, W.; Yang, F.; Hu, D.; Fang, H.; Lan, Z.; Yuan, Q., The Behavior of Hydroxide and Hydronium Ions at the Hexadecane—Water Interface Studied with Second Harmonic Generation and Zeta Potential Measurements. *Soft Matter* **2017**, *13*, 7962-7968.
- 62. Zangi, R.; Engberts, J. B. F. N., Physisorption of Hydroxide lons from Aqueous Solution to a Hydrophobic Surface. *Journal of the American Chemical Society* 2005, 127, 2272-2276.
- 63. Bob, M. M.; Walker, H. W., Effect of Natural Organic Coatings on the Polymer-Induced Coagulation of Colloidal Particles. *Colloids and Surfaces A: Physicochemical and Engineering Aspects* **2001**, *177*, 215-222.
- 64. Vermeer, A. W. P.; van Riemsdijk, W. H.; Koopal, L. K., Adsorption of Humic Acid to Mineral Particles. 1. Specific and Electrostatic Interactions. *Langmuir* 1998, 14, 2810-2819.
- 65. Xie, Q.; Li, Y.; Lv, Z.; Zhou, H.; Yang, X.; Chen, J.; Guo, H., Effective Adsorption and Removal of Phosphate from Aqueous Solutions and Eutrophic Water by Fe-Based Mofs of Mil-101. *Scientific Reports* **2017**, *7*, 3316.
- 66. Sani-Kast, N.; Labille, J.; Ollivier, P.; Slomberg, D.; Hungerbühler, K.; Scheringer, M., A Network Perspective Reveals Decreasing Material Diversity in Studies on

- Nanoparticle Interactions with Dissolved Organic Matter. Proceedings of the National Academy of Sciences **2017**, 114, E1756.
- 67. Cai, Z.; Dwivedi, A. D.; Lee, W.-N.; Zhao, X.; Liu, W.; Sillanpää, M.; Zhao, D.; Huang, C.-H.; Fu, J., Application of Nanotechnologies for Removing Pharmaceutically Active Compounds from Water: Development and Future Trends. *Environmental Science: Nano* 2018, 5, 27-47.
- 68. Sarkar, B.; Mandal, S.; Tsang, Y. F.; Kumar, P.; Kim, K.-H.; Ok, Y. S., Designer Carbon Nanotubes for Contaminant Removal in Water and Wastewater: A Critical Review. Science of The Total Environment 2018, 612, 561-581.
- 69. Pang, Y.; Yu, J.; Tang, L.; Zeng, G.; Zhu, C.; Wei, X., Chapter 1 Magnetic Nanohybrid Materials for Water-Pollutant Removal. In *Nanohybrid and Nanoporous Materials for Aquatic Pollution Control*, Tang, L.; Deng, Y.; Wang, J.; Zeng, G., Eds. Elsevier: 2019; pp 1-30.
- 70. Sun, L.; Yuan, D.; Wan, S.; Yu, Z.; Dang, J., Adsorption Performance and Mechanisms of Methylene Blue Removal by Non-Magnetic and Magnetic Particles Derived from the Vallisneria Natans Waste. *Journal of Polymers and the Environment* 2018, 26, 2992-3004.
- 71. Geiger, F. M., Second Harmonic Generation, Sum Frequency Generation, and X(3): Dissecting Environmental Interfaces with a Nonlinear Optical Swiss Army Knife. *Annual Review of Physical Chemistry* **2009**, *60*, 61-83.
- Deng, G.-H.; Qian, Y.; Rao, Y., Development of Ultrafast Broadband Electronic Sum Frequency Generation for Charge Dynamics at Surfaces and Interfaces. *The Journal of Chemical Physics* 2019, 150, 024708.
- Ebben, C. J.; Ault, A. P.; Ruppel, M. J.; Ryder, O. S.; Bertram,
 T. H.; Grassian, V. H.; Prather, K. A.; Geiger, F. M., Size-Resolved Sea Spray Aerosol Particles Studied by Vibrational Sum Frequency Generation. *The Journal of Physical Chemistry A* 2013, 117, 6589-6601.
- Roke, S., Nonlinear Optical Spectroscopy of Soft Matter Interfaces. ChemPhysChem 2009, 10, 1380-1388.